Improving the Characteristics of Two-Stage Fuel Pump by Optimizing the Blades Geometry

Oleg Baturin, Daria Kolmakova, Grigorii Popov and Vasilii M. Zubanov

Department of Aircraft Engine Theory, Samara National Research University, Samara, Russian Federation

Keywords: Screw Centrifugal Pump, Blade, CFD, Optimization.

Abstract: The article presents a refining method for a two-stage screw centrifugal pump by the joint usage of optimization software IOSO, meshing complex NUMECA and CFD software ANSYS CFX. The pump main parameters: high-pressure stage rotor speed was 13300 rpm; low-pressure rotor speed was 3617 rpm by gearbox; inlet total pressure was 0.4 MPa; outlet mass flow was 132.6 kg/s at the nominal mode. This article describes the process of simplifying the calculation model for the optimization. The parameters of camber lines of the low-pressure impeller, transition duct, and high-pressure impeller blades for two sections (hub and shroud) were chosen as optimization parameters. The optimization goal was the increase of the pump efficiency with preservation or slight increase in the pressure head. The efficiency was increased by 3%.

1 INTRODUCTION

Pumps are the integral part of both industrial production and everyday human life (Andronov, 2004), centrifugal pumps are used in water supply and disposal systems. A special place is occupied by the screw centrifugal pumps as the devices for supplying liquid components to the rocket engine. In this case, the turbo-pump unit requires both high performance and high reliability of operation. It is known (Ivanov, 2006), more than 70% of crashes of liquid propellant rocket engines occurred due to the breakdown in the turbo-pump units.

Currently used turbo-pump units for liquid propellant rocket engines (LPRE) were designed in the 1960-1970. The geometry of the pumps was projected initially by theoretical and empirical dependencies, and they were designed by expensive experimental development of the engine/pumps.

A modern CFD programs allows the simulation of the pump workflow. After validating the simulation results, these CFD models can be used to study the effect of the pump parameters on its performance. It is also possible to optimize the pump using verified CFD model as a "black box".

An optimization of the pump geometry is carried out for the following purposes:

1) improvement of the pump performance while maintaining the pump reliability.

2) providing the same pump performance with the reduced pump rotor speed. In this case, the load on the rotor elements of the turbo-pump unit will be decreased;

3) the combination of the first two approaches.

Investigation of the working process in previous studies (Zubanov, 2015; Zubanov, 2016) showed the presence of vortex zones in the high-performance pumps. The high-performance fuel pump was adopted as the study subject (Figure 1, 2).

The fuel pump main parameters with water as the working fluid (based on experiment data) were the following:

- high-pressure stage rotor speed was 13300 rpm, low-pressure rotor speed was 3617 rpm by gearbox;
- inlet total pressure was 0.4 MPa;
- outlet mass flow was 132.6 kg/s at nominal mode.

Figure 3 shows the meridional section of the fuel pump, in which vortex zones present in the following regions:

- the periphery of the inlet edge of the low-pressure screw (LPS) and high-pressure screw (HPS) (areas 1 and 4);
- the periphery of the leading edge of the low-pressure impeller (LPI) (area 2);
- the area closer to LPI stage outlet at the hub (area 3);

▪ the stagnation zone of the vortex near HPI hub (area 5).

Vortices in regions 1 and 4 are due to the design of the screws. But vortices 2, 3 and 5 in the pump are undesirable. Thus, the decrease of the intensity of vortices 2, 3, and 5 will increase the efficiency and pressure head of the pump. This can be achieved by changing the geometry of LPI, TP and HPI blades.

2 NOMENCLATURE

These are abbreviations of the pump parts (Figure 2):
▪ KID   - Knee Inlet Duct;
▪ LPS   - Low Pressure Screw passage;
▪ LPI   - Low Pressure Impeller passage;
▪ TP - Transferring Passage;
▪ HPS   - High Pressure Screw passage;
▪ HPI   - High Pressure Impeller passage;
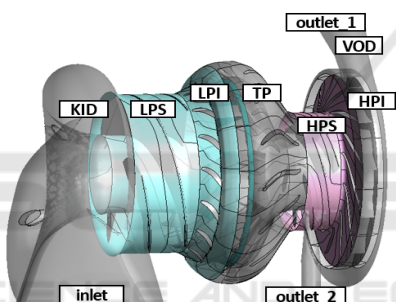▪ VOD   - Volute Outlet Duct.

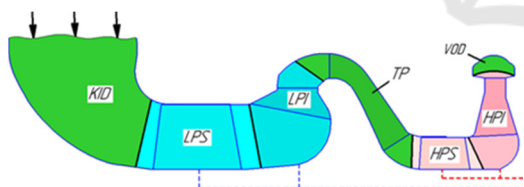Figure 1: 3D view of the pump under investigation.
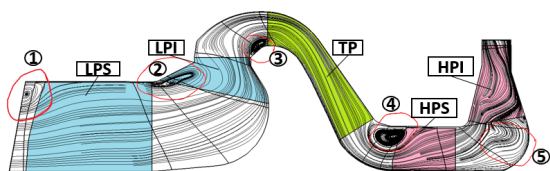

Figure 2: Meridional section of the pump.

Figure 3: The pump meridional section with vortex zones.

3 METHODOLOGY

A proven CFD model will be used from the previous study (Zubanov, 2016). Water was used as the working fluid because the experimental test data for water were available. The proven CFD model ensures a coincidence of Pressure Head value with experimental data with the accuracy of 6.9% at nominal mode, and of Internal Efficiency - 2.0%. The experimental data are presented in the form of points.

The IOSO program was used as an optimizer (IOSO, 2017). The optimization algorithm requires multiple iterations with CFD-model. The mesh model size has a direct impact on the speed of calculation. For optimization, it is important to have a mesh model with the smallest number of elements, which adequately repeats the pressure and efficiency characteristics of the pump. This article describes the process of simplifying the calculation model for the optimization. A calculation will be performed with the settings of the basic mesh model for the final optimal variant of the pump design.

The physical processes in the pump are non-stationary (Pinho, 2014; Reboud, 2003; NUMECA, 2017). While calculations in a stationary statement are sufficient for most engineering tasks, the parameters of efficiency and pressure head vary by iterations in high-performance pumps for stationary calculation. It was found in previous studies the time-averaged parameters of efficiency and pressure head for non-steady-state calculations coincide with the parameters averaged over iterations for stationary calculation. Therefore, further calculations will be carried out in the stationary statement, with averaging the last 100 iterations by a specially script. To calculate one task 600 iterations were used, while the oscillation of parameters remained constant after 400 iterations (Figure 4). The maximum level of parameter variation for the last 100 iterations was also controlled by a special script.
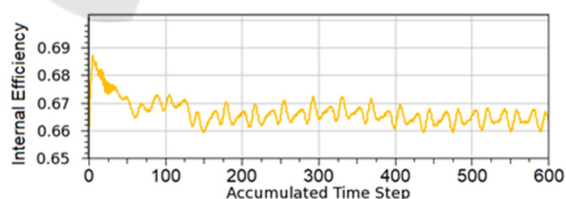

Figure 4: The internal efficiency parameter by the accumulated time step.

4 OPTIMIZATION ALGORITHM AND DESCRIPTION OF BLADE PARAMETERIZATION

IOSO software was used as optimization program (IOSO, 2017). This program has proven itself in

many research studies (Jha, 2015; Matveev, 2014; Yang, 2016). The optimization algorithm for the investigated pump is shown in Figure 5.

At each step of optimization, the optimizer *IOSO PM* generates a Vector of variable parameters x_1, x_2, x_3, …, x_n. The Vector describes the geometry of the LPI, TP and HPI blades in a parametric form. The Vector of variable parameters is transferred to the reprofiling block, at which *Numeca AutoBlade* (ANSYS CFX-Solver Modeling Guide, 2011) program perform a conversion of the blades by Vector data and save them in the form of geometry files in a *.*GeomTurbo* format. Then, the mesh model is created in the *Numeca AutoBlade 5* program using new blades. At the next step, the CFD calculation is performed with the new mesh model. The processing of CFD-results is carried out by a special script. As a result, several output files are created containing pump operation parameters in the text format. These parameters are then passed to the optimizer IOSO.

The optimization goal was the increase of the pump efficiency with preservation or slight increase in the pressure head. This will reduce the load of the main gas turbine. It is necessary because the main gas turbine of the turbopump unit operates in oxidizing environment (the mass ratio at the gas generator is more than 56 for oxygen/kerosene components).
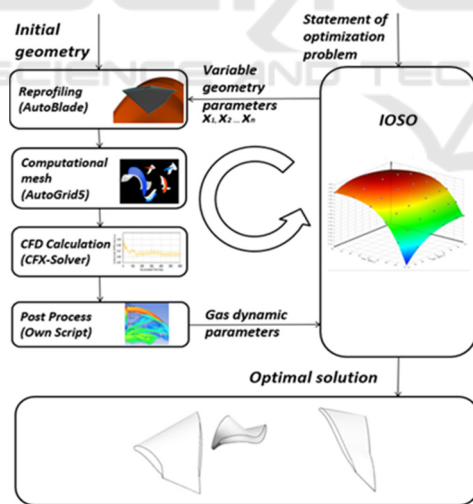

Figure 5: The optimization algorithm of the investigated pump.

The blades fitting was performed in the *Numeca AutoBlade*. The parameters of camber lines of the LPI, TP and HPI blades for two sections (hub and shroud) were chosen as optimization parameters. Figure 6 shows the parameterization scheme of the LPI blades. The camber lines of the LPI, TP and HPI

blades are described by Bezier curves. The camber line of the LPI blade is described by three points-poles, while the camber lines of the TP and HPI requires at least four point-poles. This is due to the large length of the TP and HPI blades. The distribution of the cross sections along the blade height was carried out according to the linear law. The total number of independent variables was 22.

The pump model with fitted blades was called v0, and a comparison of its characteristics with the basic values shows the pressure head differs from the basic value by 20 m, or 1%, and the efficiency differs by 0.013 or 2%. A good match of the mesh B2Bm2 level with a mesh B2B0 level is revealed.
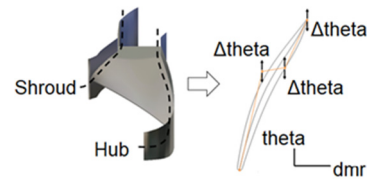

Figure 6: 2D parameterization of the LPI blades.

5 SIMPLIFICATION OF THE PUMP MODEL FOR OPTIMIZATION

Simplification of the pump model is necessary to reduce the estimated time of CFD-calculation.

Simplified models were calculated with the *Mass Flow* boundary condition, since changing the geometry of the LPI, TP, and especially of the HPI can lead to a displacement of the pump characteristics.

The simplification of the pump model included:
- comparison of the results of simulations with cavitation and without one;
- comparison of the results of stationary and transient simulations of pump workflows;
- a study of the pump characteristics behavior, depending on the mesh model level in the blades passages (B2B section) and on the flowpath amounts.

5.1 Simulations Results Comparison with Cavitation and without One

The phenomenon of cavitation should be considered in hydrodynamic investigations of the pumps, because the water hammer effect, arising from the cavitation, poses a serious risk to the pump reliability. Also, neglecting the cavitation simulation in pumps

can lead to obtaining characteristics with a sufficiently large error of 10-15% (Ding, 2011; Athavale, 2002). To estimate this error for the pump, the modeling of working processes with cavitation was carried out. The simulation was performed with the basic mesh model. Cavitation settings were the following:

- doubled fluids: primary – liquid, secondary – vapor;
- homogeneous model of multiphase;
- cavitation model of Rayleight-Plesset;
- bubbles mean diameter is 2 microns;
- saturation pressure is 3169 Pa;
- volume fraction at inlet: "1" for liquid, "0" for vapor.

The results of comparison of efficiency are shown in Figure 7. The pressure head characteristics are practically the same, and the efficiency with cavitation is lower by 1.0-2.9%.

Simulation of the pump considering cavitation took in 1.9 times more processor-hours than simulations without cavitation. The pressure and efficiency characteristics are equidistant in the near-nominal mode. Therefore, the modeling of workflows in the pump was carried out without considering cavitation for further research.
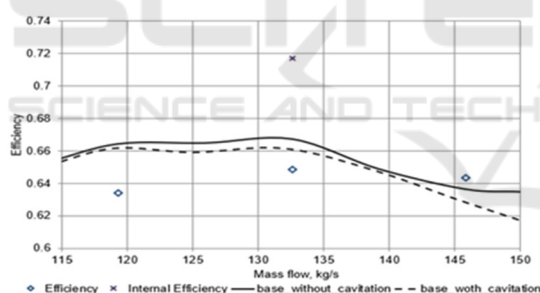

Figure 7: The internal efficiency characteristic of the investigated pump without and with cavitation modeling.

5.2 Comparison of the Results of Stationary and Transient Simulations of Pump Workflows

In the «Methodology» section, the specific decision on stationary modeling with averaging the last 100 iterations was mentioned. This section contains the rationale for such approach.

The simulation was performed with the basic mesh model. Settings for the transient modeling:

- the time step is 3.7594e-005 seconds. This value corresponds to 1/10 of the transit time of the HPI blade channel;

- Maximum Number of Coefficient Loops is 10;
- Number of Timesteps is 600.

The sustained operation of the pump required 300 iterations. The last 300 iterations (of total 600) were used for averaging the transient results.

Figure 8 show the pump efficiency for stationary and transient tasks that differ by less than 0.3%.

The simulation of non-stationary pump operation was very resource-intensive task by 2.7 times more than for the stationary simulation without cavitation. Regarding the foregoing, the simulation of working processes in the pump was carried out in the steady state without cavitation for further investigations.
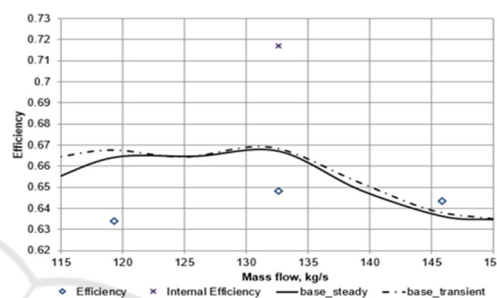

Figure 8: The internal efficiency characteristic of the investigated pump for steady and transient cases.

5.3 Investigation of the Pump Characteristics Dependence on the Mesh Model

The basic mesh model of the vane units contained 2.81 million elements with 81 flowpaths by height.

The number of elements in the B2B section of the vanes of the basic model was adopted as B2B0 level. Two levels of B2B meshes were created with a reduced number of points: B2Bm1 and B2Bm2. The B2B levels differed by ~1.3 times according to the recommendations given in (ANSYS CFX-Solver Modeling Guide, 2011; Marchukov, 2017; Jha, 2015). The number of points in 3D meshes depending on B2B level and flowpaths number, which are presented in Table 1.

Table 1: The number of points in the 3D mesh, $\times 10^6$.

B2B level	Flowpaths number			
	81	73	65	57
B2B0	3.08	2.80	2.51	2.22
B2Bm1	2.28	2.10	1.85	1.64
B2Bm2	1.77	1.60	1.44	1.27

All mesh models adequately predict the values and behavior of the pressure head and internal efficiency characteristics. Figures 9 and 10 show the

pressure head and efficiency characteristics of the investigated pump for several mesh models. The internal efficiency and pressure head values were determined at the outlet of HPI stage, to determine the influence of only the mesh parameters of the blade elements on the pump characteristics.

The maximum difference of the pressure head at the nominal mode for B2Bm2_flowpath57 mesh model was 1% relative to the basic value, and of the internal efficiency - 0.2% for the for B2B0_flowpath57 mesh model. The mesh model B2Bm2_flowpath57 was chosen for the optimization task because it provides the fastest possible solution time with the adequate prediction of the pump characteristics.
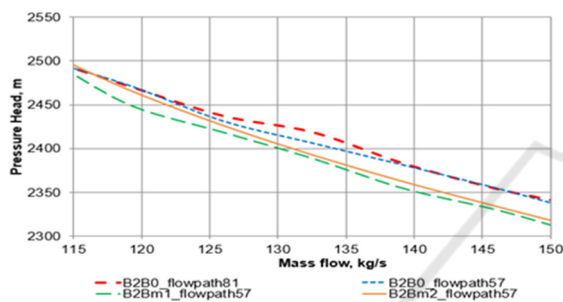

Figure 9: The pressure head characteristic of the investigated pump for several mesh models determined at the outlet of the HPI stage.
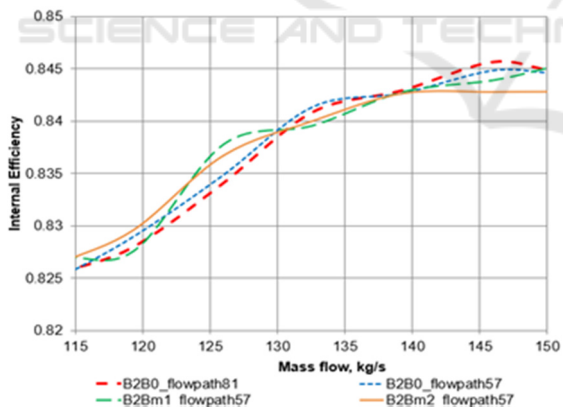

Figure 10: The internal efficiency characteristic of the investigated pump for several mesh models determined at the outlet of the HPI stage.

6 OPTIMIZATION RESULTS

The optimization task was performed using B2Bm2 mesh model of blades and mesh models of KID and VOD from rough mesh of previous study (Zubanov, 2015).

The optimization task of the pump had criteria:

- increase in the internal efficiency;
- preservation or a slight increase the pressure head.

The optimization of the pump required more than 200 iterations. The Pareto front «efficiency-pressure head» was obtained. For a detailed analysis, 2 points were selected from the Pareto front:

- v33 is the variant of the pump with increased internal efficiency by 3.3% and increased pressure head by 6.8% at B2Bm2 mesh level relative to variant v0;
- v41 is the variant of the pump with increased internal efficiency by 5.4% and increased pressure head by 0.2% at B2Bm2 mesh level relative to variant v0.

Then calculations of variants v33 and v41 were performed at B2B0 mesh level. The internal efficiency and pressure head characteristics with boundary condition *Mass Flow* at the outlet are shown in Figures 11-12. The pressure head of pump variant v41 is below the basic value at the parity level of the internal efficiency in comparison with pump variant v33. In addition, the internal efficiency of the pump is sharper in the field of high mass flows. The pump variant v33 seems preferable.

The internal efficiency of the pump variant v33 has the increased value by 3.1% and the increased pressure head by 0.4% at nominal mode relative to the basic values.

Figure 13 shows the blade-to-blade sections of LPI, TP and HPI pump blades of basic and optimized (v33) versions. LPI blade became more elongated closer to the exit, the blade of the TP became more curved, and provides a certain flow angle for the HPS. The HPI blade underwent major change closer to the outlet of HPI stage, especially at the shroud. It seems, that such shape of the HPI blade ensures compensation of Pressure Head losses in the periphery of the HPS blade.
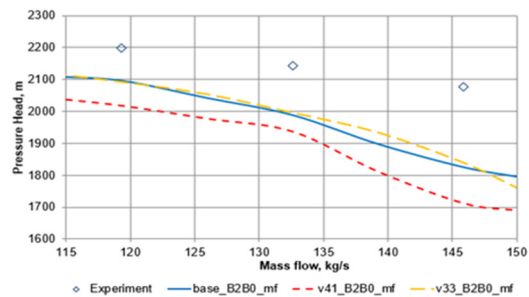

Figure 11: The pressure head characteristic of the pump with boundary condition *Mass Flow*.
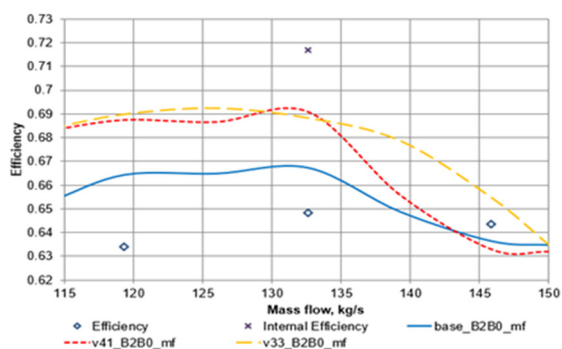
Figure 12: The internal efficiency characteristic of the pump with boundary condition *Mass Flow*.
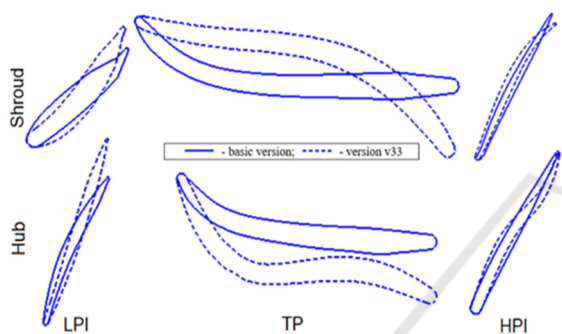

Figure 13: Blade-to-blade sections of LPI, TP and HPI pump blades of base and optimized (v33) versions.

Analysis of the pressure head and efficiency parameters by the pump parts was carried out for the basic pump, v33 and v41 variants. Changing the parameters of internal efficiency and pressure recovery coefficient is shown in Figure 14. The greatest change occurred in the TP part of the pump.

The pump variant v41 has higher efficiency for the impeller than the pump variant v33, but v41 has lower pressure recovery coefficient for the VOD. Apparently, the calculation on the fine B2B0 mesh level allowed to calculate the vortices shown in Figure 3 more detailed.

Since only the LPI, TP and HPI blades were subject to optimization, the efficiency of the LPS and HPS blades should remain at the same level or slightly change. The efficiency of the LPS blades slightly increased due to the change in the shape of the LPI blades. At the same time the efficiency of the HPS blades decreased because of the change in the velocity triangles associated with the change in the shape of the TP and HPI blades. In general, the efficiency of the pump increased by 3.1% with the increased pressure head by 0.4% due to the coordinated work of the stages (Popov, 2016).
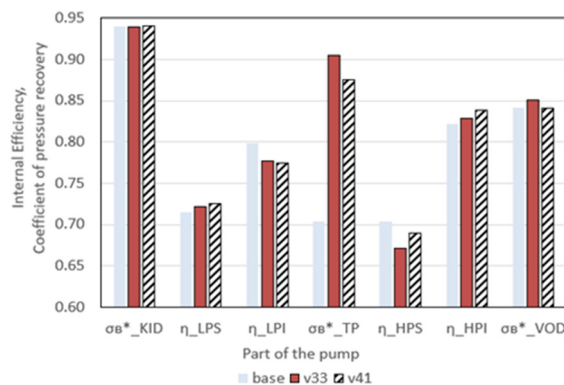

Figure 14: The parameters of internal efficiency and pressure recovery coefficient determined for the pump parts.

7 STRENGTH ANALYSIS OF HPI BLADE OPTIMAL GEOMETRY

The geometry of the HPI blades was significantly changed during the optimization. To evaluate the effect of loads acting on the optimized variant of geometry, calculations are made to determine the maximum equivalent stresses in the basic geometry and in the optimized variant of the high-pressure impeller. The calculation was carried out in ANSYS Mechanical. Computational model was the impeller sector, the cyclic symmetry condition was used. The calculation did not consider the material ductility. The pressure values on the solid surfaces were interpolated from the CFD calculation. The temperature field was 25 °C, given as constant for the entire calculation model.

As a result of the calculation of two impeller variants, the values of the maximum equivalent stresses were obtained. For the basic variant the maximum value of equivalent stress $\sigma_{\text{(von Mises stress)\_base}}$ was 961.6 MPa, for the optimized variant v33 - $\sigma_{\text{(von Mises stress)\_opt}}$ was 1038.3 MPa.

The material of HPI is chromium-nickel steel VNL-1. It has the specific stress limit of 1079 MPa (VIAM, 2017). According to J. E. Shigley «stress-concentration factors need not be employed when the material is ductile, and the loads are static» (Shigley, 2001). According to the recommendations in (VIAM, 2017) and (ANSYS Mechanical User's Guide, 2013) «failure is most often declared if yielding occurs across a complete section». Therefore, the equivalent stresses region near the maximum value was considered. A region occupying 1/4 of the maximum stress scale for each case was

adopted as such region. The equivalent stresses for the selected region was 722.3 MPa for the basic HPI blade version and 779.2 MPa – for the optimized v33 version. Then the safety factor for the basic version is 1.49, and for the optimized version is 1.38.

8 CONCLUSIONS

Two optimization studies of powerful fuel pump were performed. The first optimization task with CFD-model, which does not contain KID and VOD parts of the pump, did not allow to significantly increase the pressure head and internal efficiency. Nevertheless, optimization with the first CFD-model correctly predicted the trends in the geometry variation of the LPI and TP blades. Thus, it is possible to perform optimization of the pump blades without VOD part, while maintaining the geometry of the blades in the stage before the output device. This can be important for the gradual improvement of the pump geometry, especially if the number of variable parameters is limited by the capabilities of an optimizer program.

The second optimization task provided the pump with re-profiling geometry of the blades, which allow to obtain the increased internal efficiency by 3.1% and the increased pressure head by 0.4% at nominal mode relative to the basic values.

The strength analysis of the HPI blade was performed since the HPI blades were greatly changed at the HPI stage exit area. The maximum equivalent stresses increased by 76.7 MPa, and the safety factor of HPI decreased from 1.49 to 1.38.

The obtained reserve can be used to boost the rocket engine, and/or to reduce the loading of the main turbine, which operates in aggressive oxidizing environment.

Further optimization is planned for 3-4 sections for all blade stages, including screws. Also, conjugate optimization is planned to consider the strength model.

ACKNOWLEDGEMENTS

REFERENCES

Andronov, A. L., 2004. Features of operation of centrifugal pumps and the requirements for their electric drive. *Polzunovskii Almanac (Barnaul, Russia)*, Volume 1, pp. 150-152.

Ivanov, V. K., Kashkarov, A. M., Romacenko, E. N., Tolstikov L.A., 2006. Turbopump units for LPRE designed by NPO Energomash. *Conversion in engineering*, Volume 1, pp. 15 21.

Zubanov, V. M., Shabliy, L. S., Krivcov, A. V., 2015. Rational Technique for Multistage Centrifugal Pump CFD-Modeling. *In Proceedings of the ASME Turbo Expo*, Paper No. GT2015-42070, pp. 1-9.

Zubanov, V. M., Shabliy, L. S., Krivcov, A. V., Matveev, V. N., 2016. Technique for adequate CFD-modeling of the pump with hydro-drive of the low-pressure stage. *In Proceedings of the ASME Turbo Expo*, Paper No. GT2016-57689, pp. 1-11.

IOSO Optimization Technology. Access mode: http://www.iosotech.com.

Pinho, J., Lema, M., Rambaud, P., Steelant, J., 2014. Multiphase investigation of water hammer phenomenon using the full cavitation model. *Journal of Propulsion and Power*, Volume 30, Issue 1, January 2014, pp. 105-113.

Reboud J. L., Pouffary B., Coutier-Delgosha O., Fortes – Patella R., 2003. Numerical simulation of unsteady cavitating flows: some applications and open problems. *Fifth International Symposium on Cavitation* (CAV2003), Japan, Paper No. CAV2003-IL-10, pp. 1-10.

NUMECA. Access mode: http://www.numeca.com/en.

ANSYS CFX-Solver Modeling Guide, 2011. ANSYS Inc.

Marchukov, E. Yu., Egorov, I., Popov, G., Salnikov, A., Goriachkin, E., Kolmakova, D., 2017. Multidisciplinary optimization of the working process of uncooled axial turbine according to efficiency and strength criteria. *Proceedings of the ASME Turbo Expo*, Paper No. GT2017-64843.

Jha, R., Dulikravich, G. S., Colaço, M. J., Egorov, I. N., Poloni, C., Chakraborti, N., Fan, M., Schwartz, J., Koch, C., 2015. Multi-objective design and optimization of hard magnetic alloys free of rare earths. *Materials Science and Technology Conference and Exhibition 2015*.

Matveev, V. N., Baturin, O. V., Popov, G. M., Egorov, I. N., 2014. Seven-stage axial compressor optimization. *Engineering Optimization IV - Proceedings of the 4th International Conference on Engineering Optimization*, ENGOPT 2014, pp. 821-826.

Yang, C., Wu, H., 2016. Optimized aerodynamic design of aggressive intermediate turbine duct with strut fairings using genetic algorithms. *ASME Paper* GT2016-56639.

Ding, H., Visser, F. C., Jiang, Y., Furmanczyk, M., 2011. Demonstration and validation of a 3D CFD simulation tool predicting pump performance and cavitation for industrial applications. *Journal of Fluids Engineering, Transactions of the ASME* Volume 133, Issue 1, Article number 011101, pp. 277-293.

Athavale, M. M., Li, H. Y., Jiang, Y. U., Singhal, A. K., 2002. Application of the full cavitation model to pumps and inducers *International Journal of Rotating Machinery*, Volume 8, Issue 1, pp. 45-56.

Popov G., Goriachkin E., Kolmakova D. and Novikova Yu., 2016. Multicriteria Optimization of Axial Low Pressure Compressor of Gas Turbine Power Plant. *In Proceedings of the ASME Turbo Expo*, Paper No. GT2016-57856, pp. 1-10.

VIAM, 2017. Access mode: https://catalog.viam.ru.

Shigley J. E. and Mischke C. R., 2001. *Mechanical Enginering Design*. McGraw-Hill.

ANSYS Mechanical User's Guide, 2013. ANSYS Inc.